



ISSN: 0067-2904

Utilizing Palm Print to Identify People Based on the Resnet50 Approach

Mathiq H. Yasir, Alyaa Al-Barrak*

Department of Computer Science, College of Science, University of Baghdad, Baghdad, Iraq

Received: 31/1/2024

Accepted: 10/6/2024

Published: 30/5/2025

Abstract

In person recognition, biometrics play an important role. Behavioral or physiological characteristics are utilized by biometrics to identify an individual. Palmprint is considered highly usable and represents a reliable and unique biometric characteristic. Nevertheless, the useful and deepest features extracted from palm prints are an essential point. The most recently developed techniques use creases, wrinkles, and principal line features. However, due to closeness, these features are not enough to distinguish two individuals. Recently, one of the most important techniques that is considered a major key to extracting deep features such as texture features is deep learning. This paper proposes a biometric palm print system using the Resnet50 pre-train model to extract deep features and identify individuals. COEP and PolyU-IITD datasets are used in the simulation; moreover, the merging of COEP and PolyU-IITD in one dataset is also used. In the evaluation process, precision, F1-score, and recall are employed. The proposed system developed three models; the first model resulted in precision = 0.967, recall = 0.97, and F1 = 0.97. In comparison, the second model got precision = 0.88, recall = 0.87, and F1 = 0.86. Finally, the third model obtained precision = 0.95, recall = 0.92, and F1 = 0.93. The proposed system efficiently performs palm print identification.

Keywords: Biometric, Palm Print, COEP, PolyU-IITD, Deep Learning.

استعمال بصمة الكف للتعرف على الأشخاص بناءً على نهج Resnet50

ميثاق حسن ياسر, علياء البراك*

قسم علوم الحاسوب، كلية العلوم، جامعة بغداد، بغداد، العراق

الخلاصة

في التعرف على الأشخاص، تلعب القياسات الحيوية دوراً مهماً. يتم استعمال الخصائص السلوكية أو الفسيولوجية بواسطة القياسات الحيوية لتحديد هوية الفرد. تعتبر بصمة الكف قابلة للاستعمال بشكل كبير وتمثل خاصية بيومترية موثوقة وفريدة من نوعها. ومع ذلك، فإن الميزات المفيدة والأعمق المستخرجة من طبعة الكف هي نقطة أساسية. تستعمل التقنيات التي تم تطويرها مؤخراً للتجديد، وملامح الخطوط الرئيسية. ومع ذلك، وبسبب التشابه، فإن هذه الميزات ليست كافية للتمييز بين شخصين. حديثاً، من أهم التقنيات التي تعتبر نقطة أساسية رئيسية لاستخراج الميزات العميقة مثل ميزات النسيج هو التعلم العميق. تقترح هذه الورقة نظام بصمة راحة اليد البيومترية باستعمال نموذج التدريب المسبق resnet50 لاستخراج الميزات العميقة وتحديد الأفراد. يتم استعمال مجموعات البيانات COEP و PolyU-IITD في المحاكاة؛ علاوة على ذلك، يتم

* Email: Alyaa.al-barrak@sc.uobaghdad.edu.iq

أيضاً استعمال دمج COEP و PolyU-IITD في مجموعة بيانات واحدة. في عملية التقييم، يتم استعمال الدقة ودرجة F1 والاستدعاء. وقد طور النظام المقترح ثلاثة نماذج؛ أدى النموذج الأول إلى الدقة = 0.967، والاستدعاء = 0.972، و F1=0.976 وبالمقارنة، حصل النموذج الثاني على الدقة = 0.88، والاستدعاء = 0.874، و F1 = 0.867. وأخيراً، حصل النموذج الثالث على الدقة = 0.95، الاستدعاء = 0.92، و F1 = 0.93. يتم تحديد بصمة اليد بكفاءة باستخدام النظام المقترح.

1. Introduction

Palm print identification has been tried at various image resolutions for 15 years (high and low). Palm print recognition and security biometrics have become common. Sir William Herschel first used handprint recognition in 1858 to verify the identities of his Indian civil workers by logging their prints and comparing them to new samples on paydays. Biometrics is promising but new [1]. The utilization of palmprint modality has been deemed a crucial biometric trait in augmenting the security of an individual authentication process, encompassing both identification and verification. As a result, there has been a surge in the involvement of biometrics researchers in this field. Palm print recognition systems employ scanning devices, an application based on camera technology, and accompanying software to compare image data extracted from a palm photograph with a pre-existing record of the individual in question [2]. Palm impressions contain information similar to fingerprints. Like fingerprint scanners, palm scanners employ optical, thermal, or tactile techniques to expose the unique ridges, bifurcations, scars, wrinkles, and texture of an individual hand. These three methods are based on analyzing visible light, heat emission, and pressure. Palm sensors can be classified as either contact or contactless. The integration of palm imprints and fingerprints is frequently employed to enhance identification [3]. In criminal investigations where fingerprints are unavailable, a full or partial palm print can be taken to avoid false positives and intentional falsification. Palm prints hold more valuable information for person identification systems [4]. It has a unique trait and is permanent because it does not change. Thus, palm prints are safer than fingerprints and features. The fingerprint line minutiae feature, including ridge bifurcation and termination, gives it many handprint traits. Geometry, delta points, central lines, and creases are included. Different methods produce these traits. Palm printing has no side effects because it can be recorded on low- or high-resolution devices. It has a small footprint and a reasonable approval rate [5]. This study proposes a palm-print-based human recognition system using deep learning. Despite the rapid developments in the field of deep learning, many challenges remain. Deep learning requires very large amounts of data to train models, and it also requires high computing capabilities, including graphics and data processing.

1.1 Motivation

In criminal investigations where fingerprints are unavailable, a full or partial palmprint can be taken to avoid false positives and intentional falsification. Palmprints provide more valuable information for person identification systems [4]. It has a unique trait and is permanent because it does not change. Thus, handprints are safer than fingerprints and features. The fingerprint line minutiae feature, including ridge bifurcation and termination, gives it many handprint traits. It includes geometry, delta points, central lines, and creases. Different methods produce these traits. Palm printing has no side effects because it can be recorded on low- or high-resolution devices. It has a small footprint and a reasonable approval rate [5]. This study proposes a palm print-based human recognition system using deep learning to solve the following problem:

- Palm print authentication necessitates the extraction of palm print features before classification. In deep learning, feature extraction is self-explanatory, and machine learning is essential.

- Classification of extracted palm features, a difficulty for any authentication system, is also critical. Traditional solutions rely on lines, wrinkles, and creases that are absent due to similarity. Many complex palm features might add authenticity. Previously, palm systems relied on direct contact between the palm pattern and the capturing device, which reduced user acceptance. Current research focuses on contact-free solutions, which are more comfortable and hygienic. The gadget for acquiring high-resolution pictures, especially palm prints, may be expensive. In the acquisition module, a number of studies used low-resolution hand photographs.
- Hand deformities, tattoos, or any disease that can cause a change in some hand lines are a difficult challenge for researchers in distinguishing people through palm prints. Backgrounds in palmprint image data slow down differentiation systems by increasing their run time. After all, the images are treated on the basis that they are an array, i.e., all image boundaries are taken [6].

1.2 Challenge of palm print

- **Skin damage:** Palm joints are more significant than finger joints. Thus, palm imprints rarely distort. More critical than thumbprint distortion [2].
- **Several palm regions are represented:** Palm print quality and uniqueness vary by location [3].
- **Databases that are computational:** Palm print procedures sometimes change database coordinate systems. Spin all possible detail-matching algorithms. Palm print matching algorithms are less effective than fingerprint algorithms because palm prints have more details [4], [7].

2. Palm print Concept

Palm print recognition is a biometric identification technique that relies on the unique patterns of various features on individual palm surfaces [8]. Palm print recognition systems utilize a scanning mechanism or camera-based software, along with accompanying algorithms that analyze image data extracted from a photograph of an individual's palm and subsequently match it against an existing record for that person. Palm prints exhibit similar features to fingerprints and are amenable to comparative analysis. Palm scanners are a type of biometric technology that uses a variety of methods, including optical, thermal, and tactile techniques, to identify the unique pattern of raised areas and branches in an image of a human palm. These raised areas are called ridges, while the branches are called bifurcations. Other distinguishing features, such as scars, creases, and texture, are also considered during the scanning process [12]. The three procedures are based on visible light analysis, heat-emission analysis, and pressure analysis. Palm detectors can be classified as either contact (scanner) or contactless (camera) devices with the most palm print acquisition [13]. Figure 1 illustrates a device for capturing palm prints.



(a):Contactless palm print device

(b):Touch palm print device

Figure 1: The device for capturing palm prints a: contactless device (camera), b: contact device (scanner)

Similar to fingerprints, the surface of the palm has ridges and troughs. Palm print recognition has recently gained popularity as a result of its template database expansion [5]. Palm prints provide additional information, such as wrinkles and central lines, that can be readily extracted from low-resolution photographs. In addition, palm prints provide more information than fingerprints; thus, palmprints can be used to construct a more accurate biometric system [6].

3. Related Work

The basic steps for a palm print include image acquisition, pre-processing, extracting features, and finally matching. According to previous studies, the most important studies that evaluated datasets, including the proposed system, are listed below. (as in Table 1).

In Hannah Inbarani, 2019 [7], the approach was based on the combination of spiral features and LBP filters, with MRMR used to select the optimal features. The feature extraction process begins by dividing the image into segments, followed by skewing. Then, the kurtosis is computed for each block before calculating the vector feature using the spiral method and for classification using K-nearest neighbor. (KNN). Applying the method to handprint images from three databases.

Lavanya, H. Hannah Inbarani, 2019 [8] proposed biometric method for palmprint recognition is based on a probabilistic, crude set. Identification is based on the probability of similarity between two palmprint image characteristics. In data analysis, a probabilistic raw set is one of the primary benefits because it does not require any preliminary data information. Matching palmprints primarily relies on the feature representation of palmprint images. However, the palmprint images are converted into characteristics known as eigenpairs. These eigen palm characteristics are utilized for additional processing of eigen palm matching using a probability crude setting. Principal components analysis is employed to extract eigen palm features (Principal Component Analysis PCA). In Probabilistic Similarity-Based Rough Set, all of the features that define probabilistic similarity have been utilized in this work.

Poonia et al. 2020 [9] proposed the Delaunay Triangle Internal Angle as a palmprint template, relying on the local geometry of minute features for palmprint recognition. Delaunay triangulation is mathematically resistant to local disruptions. The template generates minutiae triplets using the minutiae transform method. These triplets also provide

interior angles and prototype handprint matches. The proposed template is resistant to palmprint reconstruction. Rotation, translation, and distortion patterns remain invariant. The proposed method improves the correct recognition rate (CRR) on PolyU, IIT-Delhi, and multispectral palmprint datasets.

In M. KADHM et al., 2021 [10], they proposed the Palmprint Recognition System (PRS). The system implemented the proposed feature extraction and classification methods with direction, Local Binary Pattern (LBP), C5.0, and Nearest Neighbor (KNN) features. The system utilized palmprint image databases from the College of Engineering Pune (COEP) and the Chinese Academy of Sciences. (CASIA).

In F. Bachay & M. Abdulameer, 2022 [11], the model includes preparation, ROI extraction, and hybrid AE+CNN feature extraction and matching. However, the COEP palmprint database has few photos, making training deep learning models that need many images challenging.

Most of the previous works are directed toward machine learning and feature extraction. This is the point at which deep learning has been resorted to, especially pre-trained models, to build a system that can distinguish people. Furthermore, previous studies have not focused on developing an integrated system with user-supported interfaces. The proposed system works on two data sets. The proposed system utilizes two global models, runs each model separately, and creates a comprehensive data set from this data to collect all cases of hand deformities caused by tattoos and writing.

Table 1: Summarize the related work

RF& year	Dataset	Method	Result
[8] 2019	-CASIA IIT Delhi COEP	-PCA -Similarity USING Euclidean Distance AND PRST	COEP Euclidean Distance ACC= 92.67
[9] 2020	Train PolyU IIT-Delhi (tested on another standard database)	-Delaunay triangulation feature vector generation	PolyU palm print EER 0.39 %, CRR= 81.125%
[10] 2021	-COEP -CASIA	KNN LBP C5.0	Accuracy COEP =99 EER=0.009 Time=9.3
[11] 2022	COEP	CNN+AI	Accuracy 97.85 F1=96.82
[16] 2019	-IITD, MS PolyU - PolyU	-LBP (Local binary pattern) k-Nearest-neighbor (KNN)	PolyU EER = 3.5 IIT Delhi ERR Left hand= 0.07 Righthand= 0.32

4. The Proposed System

The system identifying a person through palm print is a biometric system through which people are identified using a palm print, which provides advantages in preparing it to be a solid biometric system because of the unique features provided by the palm print that are not

repeated among humans. The proposed system undergoes four stages: pre-processing, data splitting for training and testing, the pre-classification stage, the classification stage, and the final stage, which involves reviewing the results and making predictions.

The proposed system is equipped with interfaces that support the user. The critical feature of the proposed system is that it consists of three models with fixed steps, where the first model is applied to the first data set and the second is applied to another different data set with the same steps. Finally, the third model is applied to a third data set formed from merging the previous two sets, and the purpose of this third model is to train all the cases that cause people not to be recognized. The following figure (2) is the proposed system diagram.

In the proposed system, work was done on two data types, where the first dataset had different cases from the second dataset. The third dataset is a comprehensive collection of all cases. The idea was to create a significant new data set containing complex cases that could cause people not to be recognized, an example of which is tattoos. The wounds are unclear snapshots as the dataset is new. It contains images from two devices, as well as two different capture methods. An explanation of the three models using three different datasets is provided below.

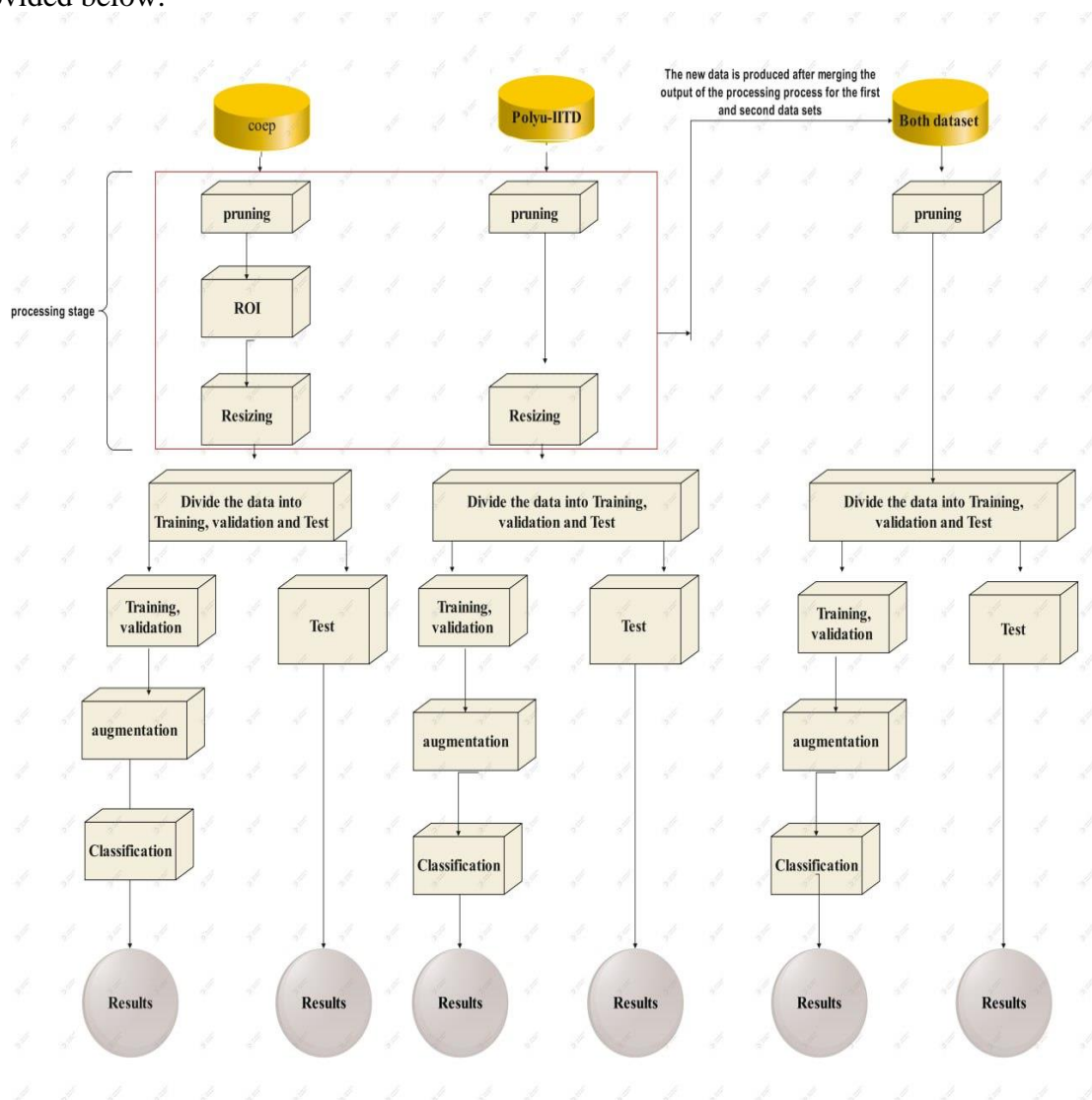


Figure 2: proposed system models

4.1 Dataset

- The COEP delegated the palmprint database for the Rajiv Gandhi Science and Technology Commission-funded project. The database contains 1344 images collected from 168 individuals. Using a digital camera, eight image samples are acquired for each subject. The image resolution is 1600 by 1200. The database was compiled over the course of one year. The images are in.jpg format, and researchers have had access to this database since 2022. Table (2) describes the COEP dataset after pruning.

Table 2: Description of COEP dataset with pruning

Size	12MB
Person	163
Image	Eight each person
Total Image	1,304 images
Type	RGB (colour image)
Dimension	1600*1200 High 1200 pixels, width 1600 pixels

- PolyU-IITD was acquired from Indian and Chinese volunteers. This is the first database collected with a general-purpose hand-held camera in multiple locations. This new palmprint database was compiled over several years from (more than) 600 subjects, making it, to the best of our knowledge, or at least until August 2020, the largest database of its kind to date. Each individual in this database has provided images of their left and right hands. As a result, this database contains images with large-scale variations from subjects. Each subject has twenty photographs aged 5 to 72 years. The subjects come from various populations, including non-officer employees, farmers, rural laborers, individuals with injured palms, and individuals with exceptional abilities or injuries. This database also contains palmprint image samples collected over fifteen years, one of its unique contributions. This dataset segments all images based on region of interest (ROI), eliminating the need for an ROI process. The details of PolyU-IITD in the proposed system are presented in Table 3.

Table 3: Description of PolyU-IITD dataset with pruning

Property	Value
Size	72.2M
Person	611
Image	For each person, two sessions 10=Right Hand 10=left hand All image (ROI)segmented
Total image	12,220
Type	RGB
Dimension	Variable

- Merge dataset used in this model, training and testing were carried out on new data resulting from the merger of the first and second datasets after the ROI process. The outcome was the creation of a new data set that included a wide variety of cases. The data set, known as PolyU-COEP, is detailed in Table 4.

Table 4: New PolyU-COEP details

Size	112MB
Person	1,385
Total image	13,524
Type	RGB
Dimension	256*256

Two datasets, COEP palmprint and PolyU-IITD, are combined into one dataset (the merged dataset) to provide all possible cases for training the system. Figure 3 is an analytical chart showing the number of images in the three datasets used to train the proposed system. Figure 4 illustrates the distribution of the dataset throughout the training and testing phases.

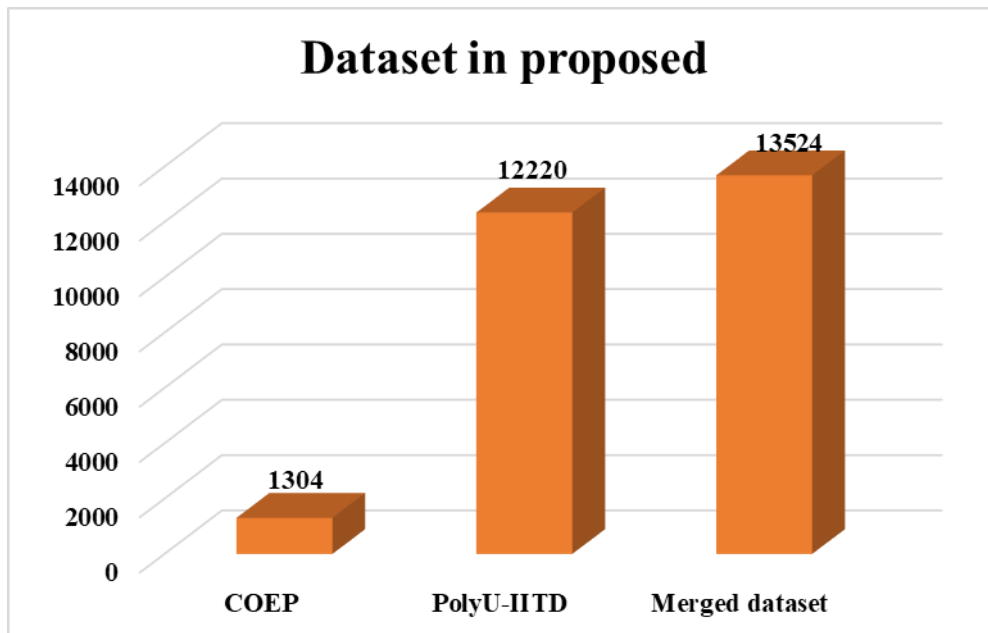


FIGURE 3: Number of images in three datasets

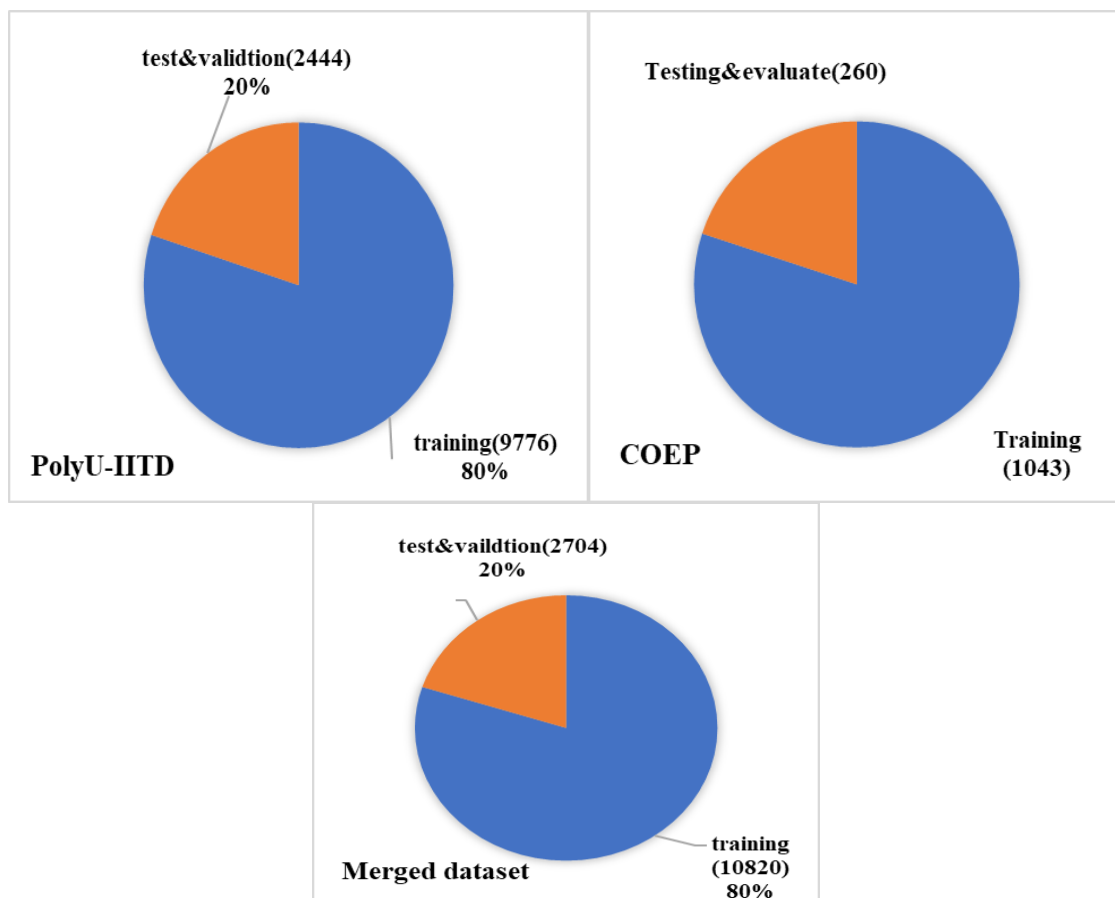


Figure 4: Dataset spilt for Training and Testing

4.2 Pre-processing

Pre-processing is an essential phase in many tasks, such as those involving text or image processing [21]. The proposed system underwent several treatment processes, which are outlined below:

- **ROI:** The first model data does not include the ROI images but includes numerous details, such as the black background and the colored dividers between the digits. These collections are not helpful to the program for palm print identification. This method was chosen for the proposed system because the objective of the system is to concentrate on the palm. These black backgrounds and colored separators help stabilize the hand during the photo shoot. These separators and backgrounds do not contribute to the proposed system because they are considered trainable features, which is untenable. Additionally, the black background is a single color, and the popularity of prominent separators can complicate system training. Therefore, the ROI operation was focused on the spacers between the digits. The ROI process is essential in the proposed system because it will shed light on the central component that needs to be improved and eliminate the components that cause training time and accuracy issues. After all, it is possible to regard these breaks as a feature and train on them, and this background that stresses the system during ROI training was beneficial. The second data set comprises customized and crop images, eliminating the need for truncation operations and defining the critical region in the second and third models. The third dataset combines the first group of subtracted images with a second group of principally cut images.

- **Resizing:** In model 1, the image sizes varied after the ROI process, causing fluctuations during the training procedure. Therefore, the third treatment step in the proposed system is to standardize the proportions of the ROI process images. The original image of the data set is large and has a very high resolution; its dimensions are 1600 by 1200 pixels, and its type is RGB with a size of 468 GB. This size is relatively large for training a neural network. When the ROI process was performed, the result was variable image sizes with high accuracy and a significant dimension; therefore, the process of unifying image sizes has been completed. As a result of the experiments, the dimensions were (256 * 256).

Moreover, in model 2, oscillation in the training process is caused by the varied image sizes resulting from the ROI process. Consequently, image size standardization is the second treatment stage in the proposed second system model. According to experiments, the process of standardizing image sizes resulted in a size of (256 * 256).

- **Data Augmentation:** Modern deep neural networks are accurate when training and test patterns match. However, this premise is often broken. Discordant train and test distributions can lower accuracy. A few experts worked on this new technology, which was adopted. (AUGMIX). Simple data handling reduces computational load and helps models withstand unexpected corruption. On arduous image classification benchmarks, AUGMIX improves robustness and uncertainty measures, sometimes more than halving the performance gap between prior methods and the best possible performance. The proposed system confines Augmentation to the training phase, employing this innovative technique to maintain accuracy measurements throughout the training process. A proposed system using AUGMIX achieves state-of-the-art robustness and uncertainty estimation while keeping or improving accuracy on standard benchmark datasets. Using stochasticity and diverse augmentations, AUGMIX achieves state-of-the-art performance by combining numerous augmented images. AUGMIX data augmentation improves training pipeline resilience, uncertainty, and slots. AUGMIX employs simple augmentation procedures and loses consistency. Stochastic sampling and layering produce varied, augmented images. Use Jensen-Shannon divergence as

a consistency loss to ensure consistent embedding across numerous augmentations of the same input image. Mixing augmentations generates robustness-inducing transformations, a standard failure mode of deep models in corruption. Fixed improvements. The model cannot be trained on hypothetical cases to handle most recognition issues. Image default issues only affect actual training.

5. Train and Evaluation

ResNet-50 is a 50-layer convolutional neural network (48 convolutional layers, one Max Pooling layer, and one average pool layer). Residual neural networks are an artificial neural network (ANN) type formed by layering residual blocks. In a proposed system that uses resnet-50, the 50-layer residuals utilize a bottleneck design for the construction block, which is a result of the trained model's architecture. A residual bottleneck block reduces the number of parameters and matrix multiplications by employing 1*1 convolutions, also known as a "bottleneck." This significantly accelerates each stratum's training. Furthermore, it employs an array of three layers as opposed to two. Moreover, this can be summed up as the Resnet50 architecture:

- 7*7 kernel convolution alongside 64 other kernels with a 2-size stride.
- A max pooling layer with a 2-sized stride.
- 9 more layers (3*3,64 kernel convolution, another with 1*1, 64 kernels, and a third with 1*1, 256 Kernal) these three layers are repeated three times.
- 12 more layers (1*1, 128 kernel, 3*3, 128 kernel, and 1*1, 512 kernel) iterated 4 times.
- 18 more layers (1*1, 256 Kernal, and 2 Kernal 3*3, 256, and 1*1, 1024 Kernal) were iterated 6 times.

The proposed system consists of three models, each with a data set for evaluating the work's efficacy. The confusion matrix [23] [24] serves as the basis for this evaluation. It is used with the test part to evaluate the work and compare it to previous works, as well as to determine the results of the proposed system and the improvements made to achieve high accuracy. Figure 4 shows the measures that were used in evaluating the three models and formulations.

The equation below shows the measures that were used in evaluating them: TN stands for true negative, which indicates the number of accurately classified negative examples [25]; TP stands for true positive, which indicates the number of accurately classified positive examples; FP stands for false positive value, which is the number of actual negative examples misclassified as positive; and FN stands for false negative value, which is the number of actual positive examples misclassified as harmful.

$$\text{Accuracy} = \frac{\text{TP}+\text{TN}}{\text{TP}+\text{FP}+\text{FN}+\text{TN}} \quad (1)$$

$$\text{Precision} = \frac{\text{TP}}{\text{TP}+\text{FP}} \quad (2)$$

$$\text{Recall} = \frac{\text{TP}}{\text{TP}+\text{FN}} \quad (3)$$

$$\text{F1_Measure} = \frac{2*\text{Precision}*\text{Recall}}{\text{Precision} + \text{Recall}} \quad (4)$$

Table 5: Summarized 50-layer Resnet in the proposed system

Name	Job
Input layer	Artificial input neurons bring initial data into a neural network for processing by successive layers of artificial neurons. Artificial neural networks start with the input layer.
ReLU layer	Avoiding vanishing gradient problem and better computation
Dropout layer	Random drop input units are used to reduce the model capacity and reduce overfitting. The proposed system's dropout value is equal to (0.2) .This value was chosen based on trial and error.
Weight decay layer	reduce model variance and the minimization overfitting, equal value (0.1). This value was chosen based on trial and error.
In the proposed system, the two were used together due to the occurrence of overfitting, and to control it, they were used together due to the nature of the input data of the variable nature.	
SoftMax layer	Calculate the probability of distribution of the event over the different events.
convolutional layer	It is the building block of CNN. It contains a set of filters (or kernels), the parameters of which are to be learned throughout the training. The size of the filters is usually smaller than the actual image. Each filter convolves with the image and creates an activation map.
Max pooling	It is a pooling operation that calculates the maximum value for patches of a feature map and uses it to create a down-sampled (pooled) feature map. It is usually used after a convolutional layer.
Zero padding	It is the process of symmetrically adding zeroes to the input matrix. It is a commonly used modification that adjusts the input size to requirements.
Batch norm	It is to take the outputs from the first hidden layer and normalize them before passing them on as the input of the next hidden layer.
Average pooling	calculating the average for each patch of the feature map. This means that each 2×2 square of the feature map is down-sampled to the average value in the square.
Flattening	collapses the spatial dimensions of the input into the channel dimension
Fully Connected	operates on a flattened input where each input is connected to all neurons
Optimizer	Optimizers adjust neural network properties like learning rate and weight decay. Thus, it increases accuracy and decreases loss. However, it is not easy to pick model weights. Thus, the proposed system selected the model with stander weights. Because Adaptive Moment Estimation blends RMSprop (root-mean-square prop) and momentum-based GD, the proposed system uses the ADIM optimizer. Momentum GD ability to store updated history and RMSprop adaptive learning rate strengthen Adam's optimizers.

5.1 Result of The First Model

This model employs the COEP dataset, and to evaluate this model using measurement of confusion matrices, this measure's standard parameter will be replaced with the confusion matrix measures. The resulting values will be obtained, and these values will be evaluated in two ways, with and without augmentation data, to demonstrate the significance of this step. First, Tables (6) and (7) display the results of the standard parameter.

Table 6: The result of the first model without augmentation

	Predict	
Actual	TP (64)	FN (1)
	FP (3)	TN (62)

Table 7: The result of the first model with augmentation

	Predict	
Actual	TP (62)	FN (5)
	FP (2)	TN (61)

Note from the above two tables that the TP values, which mean that the cases were recognized correctly, are higher in the presence of augmentation, and FP, FN, and TN are lower than in augmentation. Notice the difference when applying the following metrics in Table 8.

Table 8: Results of metrics in the confusion matrix in Model 1

<i>Result of model two without Augmentation</i>		
<i>Precision</i>	<i>Recall</i>	<i>F1</i>
$TP/TP+FP$ (64/66) = 0.961	$TP/TP+FN$ (64/ (67)) = 0.968	$2 * Precision * Recall / (Precision + Recall)$ $2 * 0.961 * 0.968 / (0.961 + 0.968)$ = 0.964
<i>Result of Model Two with Augmentation</i>		
<i>Precision</i>	<i>Recall</i>	<i>F1</i>
$TP/TP+FP$ 65/67 = 0.984	$TP/TP+FN$ 64/66 = 0.977	$2 * Precision * Recall / (Precision + Recall)$ 1.922/1.961 = 0.98

5.2 Result of The Second Model

This model uses the PolyU-IITD dataset, and to evaluate this model using measurement of confusion matrices, this measure has a stander parameter; replacing it with the confusion matrix measures, we get the results of the values, and these values will be reviewed in two ways: with the presence of augmentation data and with the lack of them, to show the importance of this step. Tables (9) and (10) show the stander parameter results.

Table 9: The result of the second model without augmentation model 2

	Predict	
Actual	TP (582)	FN (33)
	FP (29)	TN (577)

Table 10: The result of second model with augmentation model two

	Predict	
Actual	TP (591)	FN (29)
	FP (20)	TN (582)

Note from the above two tables that the TP values, which mean that the cases were recognized correctly, are higher in the presence of augmentation, and FP, FN, and TN are lower than in augmentation. Moreover, that is fine. However, notice the difference when you apply the following metrics in Table (11).

Table 11: Results of metrics in confusion matrices in the second model

<i>Result of model two without Augmentation</i>		
<i>Precision</i>	<i>Recall</i>	<i>F1</i>
$TP/TP+FP$ 1056/1222 = 0.863	$TP/TP+FN$ 1056/1246 = 0.847	$2 * Precision * Recall / (Precision + Recall)$ 1.461/1.71 = 0.854
<i>Result of Model Two with Augmentation</i>		
<i>Precision</i>	<i>Recall</i>	<i>F1</i>
$TP/TP+FP$ 1078/1222 = 0.881	$TP/TP+FN$ 1078/1231 = 0.875	$2 * Precision * Recall / (Precision + Recall)$ 1.541/1.756 = 0.877

5.3 Result of The Third Model

This model uses a merged dataset, and to evaluate this model using measurement of confusion matrices, this measure has a stander parameter; replacing it with the confusion matrix measures, we get the results of the values, and these values will be reviewed in two ways: with the presence of augmentation data and with the lack of them, which shows the importance of this step. Tables (12) and (13) show the results for the stander parameter.

Table 12: The result of the third model without augmentation, model 3

Actual	Predict	
	TP (605)	FN (6)
	FP (69)	TN (668)

Table 13: The result of the third model with augmentation model 3

Actual	Predict	
	TP (608)	FN (6)
	FP (68)	TN (670)

Note from the above two tables that the TP values, which mean that the cases were recognized correctly, are higher with the presence of augmentation, and FP, FN, and TN are lower with augmentation. Moreover, that is fine. However, notice the difference when applying the following metrics in Table 14.

Table 14: Results of the third model's metrics in confusion matrices

<i>The result of model three without Augmentation</i>		
Precision	Recall	F1
$\frac{TP}{TP+FP}$ $\frac{605}{674}$ $= 0.93$	$\frac{TP}{TP+FN}$ $\frac{608}{672}$ $=0.90$	$2 * \text{Precision} * \text{Recall} / (\text{Precision} * \text{Recall})$ $\frac{1.478}{1.720}$ $= 0.92$
<i>Result of model three with Augmentation</i>		
Precision	Recall	F1
$\frac{TP}{TP+FP}$ $\frac{608}{676}$ $= 0.951$	$\frac{TP}{TP+FN}$ $\frac{608}{664} =0.925$	$2 * \text{Precision} * \text{Recall} / (\text{Precision} * \text{Recall})$ $\frac{1.759}{1.876}$ $= 0.937$

6. Conclusion

At this time, there is an urgent need to find a biometric system to identify people. Palm print is one of the most popular topics that researchers have investigated. Furthermore, numerous studies have been conducted on the topic. In this research, we proposed a biometric system to identify people through palm prints. This system was based on two global datasets, and we created a new dataset to train on common issues faced by previous systems, such as wounds, tattoos, and blurry images. We worked on the system through several stages and multiple models. Data augmentation, which trained the data on non-existent cases, was a critical process that improved the training results. The test was conducted on three different data groups. The accuracy of the first model was 98.5%, the second model was 88%, and the third model was 95%. The results were promising, and in future work, we recommend testing an untrained dataset. A future suggestion is to work on manually collected data in a way that logically simulates reality.

Abbreviations

Symbol	Description	Symbol	Description
DL	Deep Learning	CNN	Convolution Neural Network
ERR	Error Rate Ratio	AI	Artificial Intelligence
FP	False Positive	ROI	Region Of Interest
FN	False Negative	TN	True Positive
LBP	Local Binary Pattern	TN	True Negative

References

- [1] S. Len, T. Xu, and X. Yin, "Region of interest extraction for palmprint and palm vein recognition," In 2016 9th International Congress on Image and Signal Processing, Biomedical Engineering and Informatics (CISP-BMEI), Vol.11, pp.538-542, oct.2016.doi.org/10.1109/CISP-BMEI.2016.7852769
- [2] L. Fei, B. Zhang, W. Jia and D. Zhang. "Feature extraction for 3-D palmprint recognition,": A survey. IEEE Transactions on Instrumentation and Measurement, pp.645-656, Jan.2020. doi.org/10.1109/TIM.2020.2964076
- [3] A. Mouad and A. T. Gaikwad, "Multimodal biometrics enhancement recognition system based on the fusion of fingerprint and Palmprint,": a review. Global Journal of Computer Science and Technology, Vol.16, pp.13-26, Sep.2016.
- [4] M. Ali, C. Salman and H. Aedan, "Palm print recognition based on the harmony search algorithm,". International Journal of Electrical & Computer Engineering (2088-8708), Vol.11, No.5 , pp.4113-4124, oct.2021.[doi/ 10.11591/ijece.v11i5](https://doi.org/10.11591/ijece.v11i5)
- [5] L. Wu, Y. Xu and L. Fei, "Triple-type feature extraction for palmprint recognition," , Vol.21, No.14, pp.4896, jul.2021. doi.org/10.3390/s21144896
- [6] A. K. Jain, S. Pan Kanti, S. Prabhakar, L. Hong and A. Ross, "Biometrics: a grand challenge,". In Proceedings of the 17th International Conference on Pattern Recognition, Vol.2, pp.935-942, Aug.2004. [Doi: 10.1109/ICPR.2004.1334413](https://doi.org/10.1109/ICPR.2004.1334413).
- [7] M. Ashish, "Multimodal biometrics it is: need for future systems,". International journal of computer applications, Vol. 3, No.4, pp.28-33, jun.2010.
- [8] M. Ali, V. Mahale and A. Gaikwad, "Palmprint recognition process and techniques,". International Journal of Applied Engineering Research, Vol. 13, No. 10, pp.7499-7507,2018.
- [9] A. Iula and D. Nardiello, "3-D ultrasound palmprint recognition system based on main lines extracted at several under-skin depths,". IEEE Transactions on Instrumentation and Measurement, Vol. 68, No. 12, pp. 4653-4662, Mar. 2019. [Doi: 10.1109/TIM.2019.2900177](https://doi.org/10.1109/TIM.2019.2900177)
- [10] B. Kuhn, S. Bellot, T. Couvreur, L. Dransfield, S. Henderson, A. Schley, G. Chomicki, and S. Hiscock, "A robust phylogenomic framework for the calamoid palms,". Molecular Phylogenetics and Evolution, Vol.157, p.107067, Apr.2021. doi.org/10.1016/j.ympev.2020.107067
- [11] A. Morales, M. Ferrer and A. Kumar, "Towards contactless palmprint authentication,". IET computer vision, Vol.5, No.6, pp.407-416, Aug.2011. [Doi: 10.1049/iet-cvi.2010.0191](https://doi.org/10.1049/iet-cvi.2010.0191)
- [12] S. Kadhm and T. Hasan, "Analysis of techniques and approaches to palm print,". International Journal of Nonlinear Analysis and Applications, Vol.13, no.2, pp.887-898, Jul.2022, [doi:10.22075/IJNAA.2022.6439](https://doi.org/10.22075/IJNAA.2022.6439).
- [13] M. Ali, V. Mahale, V. Yannawar and A. Gaikwad, "Palmprint recognition process and techniques," International Journal of Applied Engineering Research, Vol.13, No.10, pp.7499-7507,2018.
- [14] W. Wu, S. Elliott, S. Lin, S. Sun, and Y. Tang, "Review of palm vein recognition," IET Biometrics, Institution of Engineering and Technology, pp. 1–10, Jan.2020. [Doi 10.1049/iet-bmt.2019.0034](https://doi.org/10.1049/iet-bmt.2019.0034).
- [15] Hussies, J. Liu-Jimenez, I. Goicoechea-Telleria and R. Sanchez-Reillo, "A survey in presentation attack and presentation attack detection,". International Carnahan Conference on Security Technology (ICCST), Vol.9, No.1, pp.1-13, Oct.2019. [DOI: 10.1109/CCST.2019.8888436](https://doi.org/10.1109/CCST.2019.8888436).

- [16] B. Attallah, A. Serir and Y. Chahir, "Feature extraction in palmprint recognition using spiral of moment skewness and kurtosis algorithm,". Pattern Analysis and Applications, No.22, pp.1197-1205. Aug.2019 doi.org/10.1007/s10044-018-0712-5.
- [17] B. Lavanya and H. Inbarani, "Palmprint Identification Based on Probabilistic Rough Sets,". International Journal of Scientific & Technology Research, Vol.8, No.10, pp.992-1000, Oct.2019.
- [18] P. Poona, K. Ajmera and V. Shende, "Palmprint recognition using robust template matching,". Procedia Computer Science, Vol.167, pp.727-736,2020. doi.org/10.1016/j.procs.2020.03.338
- [19] M. Kadhm, H. Ayad, and J. Mohammed, "Palmprint recognition system based on proposed features extraction and (c5.0) decision tree, k-nearest neighbor (KNN) classification approaches,". J. Eng. Sci, Vol.16, No.1, pp.816-831, Feb.2021.
- [20] F. Bachay and M. Abdul Ameer, "Hybrid Deep Learning Model Based on Autoencoder and CNN for Palmprint Authentication", Vol.15, No.3, May.2022. [DOI:10.22266/ijies2022.0630.41](https://doi.org/10.22266/ijies2022.0630.41).
- [21] A. Hussien and N. Abdullah, "A Review for Arabic Sentiment Analysis Using Deep Learning,". Iraqi journal of Science, Vol. 64, no. 12, pp. 65726585, 2023. [DOI:10.24996/ijis.2023.64.12.37](https://doi.org/10.24996/ijis.2023.64.12.37).
- [22] N. Hussein and B. Al-Sarray. "Deep Learning and Machine Learning via a Genetic Algorithm to Classify Breast Cancer DNA Data,". Iraqi Journal of Science.Vol.63, no.7, Jul. 2022 pp.3153-68.[DOI: 10.24996/ijis.2022.63.7.36](https://doi.org/10.24996/ijis.2022.63.7.36)
- [23] Abood, Q.K., 2023. Predicting Age and Gender Using AlexNet. TEM Journal, 12(1) Vol.12, Issue 1, pp 512-518, Feb. 2023, [DOI: 10.18421/TEM121-61](https://doi.org/10.18421/TEM121-61).
- [24] A. IJAZ, B. RAZA, I. KIRAN, A. WAHEED, A. RAZA, H. SHAH and S. AFTAN, "Modality Specific CBAM-VGG Net Model for the Classification of Breast Histopathology Images via Transfer Learning," IEEE Access, vol. 11, pp.15750-15762, Feb.2023.[Doi: 10.1109/ACCESS.2023.3245023](https://doi.org/10.1109/ACCESS.2023.3245023)
- [25] Al Tamimi, R.N.M., DEEP LEARNING TECHNIQUES FOR SKULL STRIPPING OF BRAIN MR IMAGES.